University of Glasgow | Experimental Particle Physics

GLAS-PPE/2008-25
25th October 2008

Department of Physics and Astronomy
Experimental Particle Physics Group
Kelvin Building, University of Glasgow,
Glasgow, G12 8QQ, Scotland
Telephone: +44 (0)141 330 2000 Fax: +44 (0)141 330 5881

Radiation Hardness Tests of Double-Sided 3D Detectors

David Pennicard[1], Celeste Fleta[1], Giulio Pellegrini[2], Manuel Lozano[2],
Richard Bates[1], Chris Parkes[1], Lars Eklund[1] and Tomasz Szumlak[1]

[1] University of Glasgow, Department of Physics and Astronomy, Glasgow, UK, G12 8QQ
[2] Instituto de Microelectronica de Barcelona, IMB-CNM-CSIC, 08193 Bellaterra, Barcelona, Spain

Abstract

3D detectors are potentially useful for future high-luminosity colliders such as the SLHC, due to their radiation hardness. IMB-CNM have fabricated a set of 3D detectors that use a "double sided" 3D structure, where the two sets of electrode columns are etched from opposite sides of the substrate, and do not pass through the full substrate thickness. Simulations show that this structure should give similar radiation hardness to the standard full-3D structure. Two sets of devices have been successfully tested; Medipix2 pixel detectors and strip detectors coupled to LHC-speed readout electronics. The unirradiated 3D Medipix2 detectors have shown extremely low operating voltages and low charge sharing in tests with X-rays, and the strips have shown relatively high charge collection at high levels of radiation damage.

IEEE Nuclear Science Symposium
Dresden, 2008

1 Introduction

1.1 3D detectors and radiation hardness

A 3D detector [1] is a variety of photodiode detector that has an array of n- and p-type electrode columns passing through the thickness of a silicon substrate. By using this structure, it becomes possible to combine a standard substrate thickness of a few hundred microns with a lateral spacing between electrodes up to a factor of ten smaller. So, the depletion and charge collection distances are dramatically reduced, without reducing the sensitive thickness of the detector. This means that the device has extremely fast charge collection and a low operating voltage. The short collection distance and the electric field pattern in the device also will reduce the amount of charge diffusion between adjacent pixels, resulting in lower charge sharing [2].

These advantages should make 3D detectors substantially more radiation-hard than standard photodiodes. When high-energy particles pass though silicon, they collide with atoms and create defects in the crystal lattice, altering the material's behaviour [3]. Firstly, certain defects act as p-type dopants. At high fluences, the effective doping concentration in the device will become large, greatly increasing the depletion voltage. (In most n-type substrates, type inversion will also occur.) Due to their small electrode spacing, it should still be possible to fully deplete radiation-damaged 3D detectors at a reasonable voltage. Secondly, defects can trap the free electrons and holes generated by ionizing radiation, preventing them from being collected within the readout chip's integration time and hence reducing the collection signal. A 3D detector has a short collection distance, and will have a high electric field at a moderate bias voltage, leading to fast collection and reduced charge trapping. Additionally, the 3D detector's low charge sharing will improve the chances of getting a single, unambiguous hit on the detector.

1.2 3D detectors for high-luminosity colliders

An upgrade to the Large Hadron Collider at CERN, named "Super-LHC" [4], is planned for around 2017. This upgrade will increase the collider's luminosity by a factor of 10. The increase in the number of collisions should increase the number of events involving rare production and decay processes, allowing more accurate measurements of the properties of the Higgs (or any new physics discoveries), and also effectively extending the experiment's mass reach. However, detectors at the SLHC will need to cope with the corresponding increase in the radiation damage they receive.

The radiation dose received by the detectors decreases with distance from the interaction point. The innermost layer of the ATLAS pixel detector (the "b layer") [5] will be at a radius of just 5cm, and will receive an extremely high radiation fluence of around 1×10^{16} 1MeV-n$_{eq}$/cm^2 over the SLHC's running time [6]. Due to their radiation hardness, 3D detectors are a promising technology for this inner pixel layer. 3D detectors are also being considered for the b-layer replacement in 2012 [7]. Before using 3D detectors in a practical experiment, however, it is necessary to optimise their design, and establish a sufficiently reliable fabrication process.

2 Double-sided 3D detectors at IMB-CNM

2.1 Device structure and fabrication

The 3D detectors tested here have been fabricated at IMB-CNM in Barcelona. They use an alternative, "double sided" 3D structure [8]. This is illustrated in Fig. 1. In this structure, electrode columns of one type are fabricated from the front surface and used for readout, and the second set of columns is fabricated from the back side and used for biasing. Neither set of columns passes through the full thickness of the substrate, which makes the fabrication process somewhat easier; in particular, no support wafer is needed. In this first set of devices fabricated by IMB-CNM, the columns are 250μm long and 10μm in diameter. The substrate is 300μm-thick n-type silicon, and the readout columns etched from the front surface are p-type, to avoid the need for electrode isolation.

The column fabrication process requires specialised micromachining equipment. First, deep holes are etched in the silicon, using Inductively Coupled Plasma etching. This involves a two-stage cycle of etching and passivation. Initially, fluorine ions are driven down into the wafer, etching away the base of the hole. After several seconds of this, the machine switches to using C_4F_8, which forms a protective coating on the inner surfaces of the hole. This prevents the sides of the hole from widening during the next etching cycle. After the columns are etched, the interior of the columns and the surface of the wafer are coated with 3μm of polysilicon. The columns are then doped through the polysilicon, using diffusion from a solid source. On the back surface, this doped polysilicon layer will connect all the bias columns together, whereas on the front surface the polysilicon

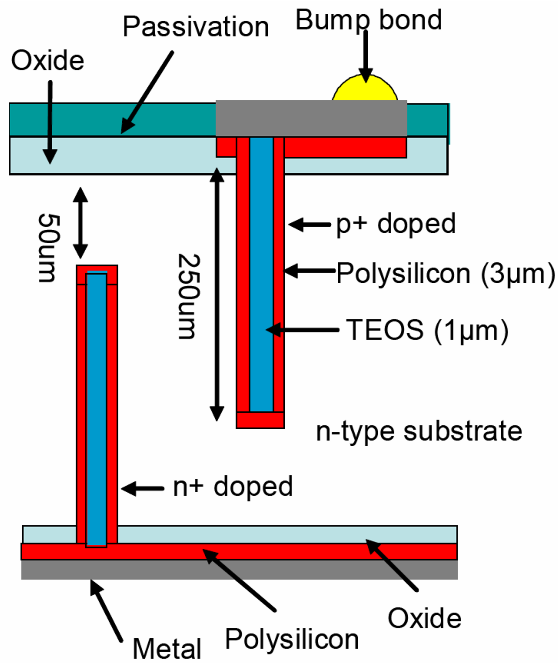

Figure 1: Diagram of the double-sided 3D structure produced by IMB-CNM.

must be selectively etched to separate the readout columns. Finally, the interior of the columns is passivated with silicon dioxide, using TEOS. This process needs to be repeated to form the two sets of columns.

2.2 Simulated behaviour

In reference [9], the expected behaviour of these double-sided 3D detectors is investigated using the Synopsys TCAD simulation package [10]. The key point is that throughout most of the device volume, where the 250μm-long columns overlap, the electric field behaviour matches that of a standard 3D detector. The double-sided structure only behaves differently around the very front and back surfaces of the detector, where the electric field becomes weaker. This can be seen in Fig. 2, which shows the electric field around the front surface of the detector, using a vertical cross-section passing through adjacent n+ and p+ columns. (The simulation uses 100V bias, and a pixel size of 55μm to match the Medipix2 detectors discussed later.) Charge deposited in these weaker-field regions will be collected more slowly, and will suffer from higher charge trapping following radiation damage.

However, the double-sided 3D structure makes it possible to use a substrate thickness greater than the column length. Since there are practical limitations on how deep the electrode columns can be made for a given column diameter, this means that the double-sided detector can have a greater sensitive thickness than the equivalent full-3D detector, which will increase the signal size somewhat. To test this, the charge collection with minimum ionizing particles was simulated for a double-sided 3D detector with 250μm columns and a 300μm substrate, and for a full-3D detector with 250μm columns and 250μm substrate. (Note that these simulated devices used n-type readout and p-type substrates, to match the signal polarity of the ATLAS readout chip.) These simulations were done at a variety of radiation damage levels, using the model described in [11], and a bias of 100V. The results are shown in Fig. 3. It can be seen that at low fluences the double-sided detector has slightly greater collection than the full-3D detector, due to the increased substrate thickness. At high fluences, the charge collection becomes much the same for both detectors.

2.3 Devices tested

IMB-CNM's first double-sided 3D fabrication run consisted of two 4-inch n-type wafers. The wafers contained a variety of devices and test structures, but two main sets of devices have been tested. Firstly, a set of Medipix2 pixel detectors have been tested with X-rays, to establish that the 3D devices can be successfully bump-bonded to readout chips and to test the detectors' performance before irradiation. Secondly, strip detectors connected to LHC-speed readout electronics have been irradiated and tested with MIPs to investigate their radiation hardness.

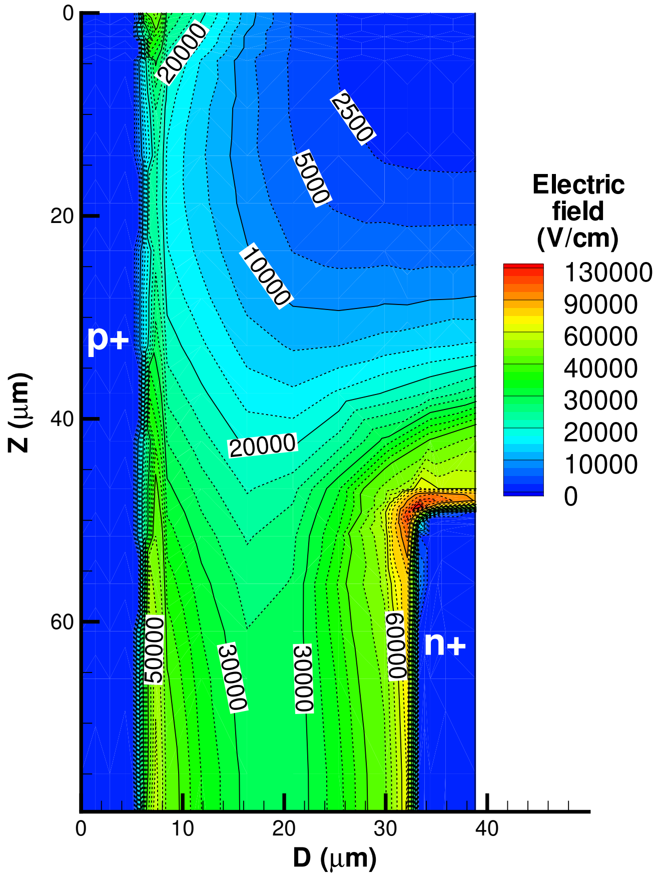

Figure 2: Simulated electric field strength around the front surface of a double-sided 3D detector at 100V bias.

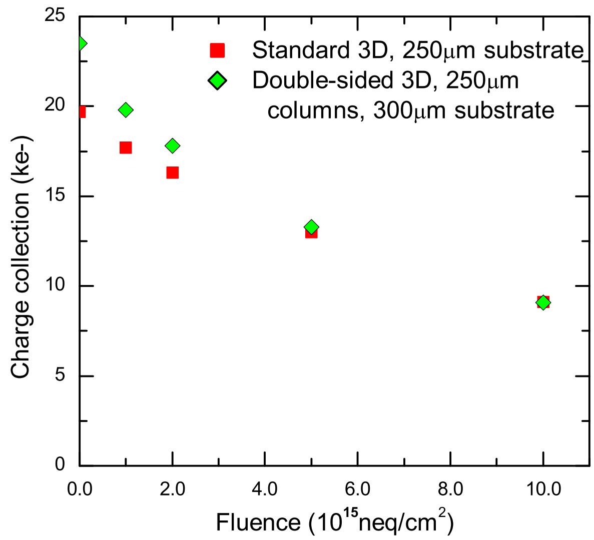

Figure 3: Simulated charge collection efficiency in double-sided and full 3D detectors with 250μm columns. The simulations use 100V bias.

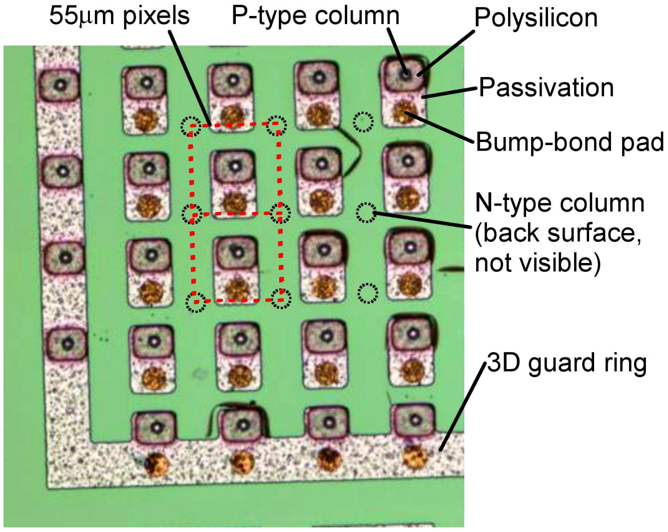

Figure 4: Photo of the front surface of a Medipix2 3D detector. The positions of the n-type columns etched from the back surface (at the corners of each pixel) have been indicated by circles.

3 X-ray tests with unirradiated 3D Medipix2 pixel detectors

The Medipix2 3D detectors consist of a 256 × 256 array of 55μm square pixels. Figure 4 shows a photograph of the surface of one of the detectors after fabrication. The tops of the p-type columns are visible, in the centre of a raised region of polysilicon (which is covered in a passivation layer). Next to each readout column, there is a metallised pad which is used for bump-bonding the sensor to the readout chip. The n-type columns fabricated from the back surface aren't visible, but their positions at the corner of each pixel are indicated by circles.

The Medipix2 chip is designed to detect X-rays, and works in a single-photon-counting mode [12]. Each hit on a pixel is compared to a pair of adjustable thresholds, and if the signal amplitude falls between the thresholds then a counter within the pixel is incremented. So, the chip counts the number of hits on each pixel during the acquisition time, giving an image without any electronic noise present.

Three 3D detectors were bump-bonded to Medipix2 readout chips at VTT, and mounted on chipboards. These assemblies were read out using the Medipix2 USB interface developed by IEAP, Czech Technical University, Prague [13]. As a preliminary test, images were taken with each detector using a 60kV tungsten X-ray tube. For example, Fig. 5 shows an image taken with a PCB placed between the tube and the detector. It was found that all three detectors worked successfully. However, two of the detectors had dead pixels along an edge—this can be seen along the left-hand side of the test image. This means that some of the bump-bonds have not made proper contact between the sensor and the readout chip. The bump-bonding process requires both chips to be very flat, and VTT reported that they measured some bowing on the sensor wafer. This might have occurred during the polysilicon deposition process, which stresses the wafer.

3.1 Depletion behaviour

As demonstrated by simulation [9], a double-sided 3D detector is expected to deplete in two stages. Initially, the depletion region will appear around the edge of each cylindrical readout column. As the bias is increased, the depletion region will grow laterally outwards until it reaches the adjacent bias columns. Due to the small lateral spacing between electrodes, this should only require about 2V in a high-resistivity substrate. At this point, most of the device volume (the 200μm central region where the columns overlap, and the region around the surface) will be depleted. However, to deplete the region around the back surface of the device, the depletion region has to grow downwards from the tip of the readout column. This requires a higher bias of around 8V in the simulation.

As a test of the depletion behaviour, a Medipix2 3D detector was illuminated with the 60kV X-ray tube, and the count rate on the detector was measured as the bias was varied. See reference [14]. The results are shown in Fig. 6. Since the Medipix2 detector has a relatively long peaking time, of order 100ns [12], any ballistic deficit is expected to be small and hence the count rate should reflect the depleted volume of the device. The count rate is seen to increase extremely rapidly over the first 2V or so, and saturates around 9V. So, this is in good agreement with the expected behaviour, and demonstrates that the detector can operate at extremely

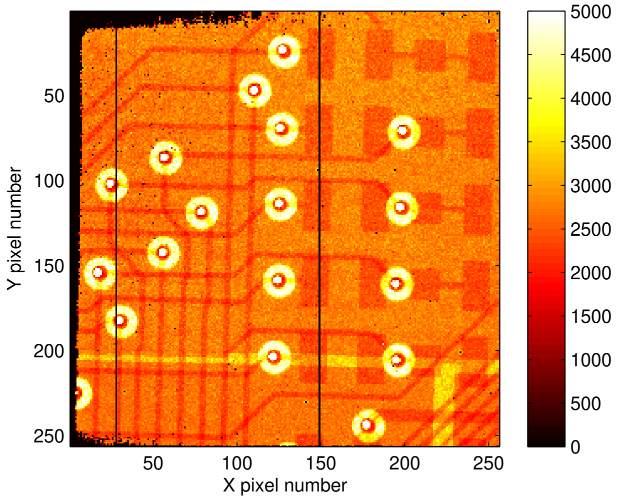

Figure 5: Image of a PCB, taken using a Medipix2 3D detector and a 60kVp X-ray tube, using a threshold energy of about 20keV. The number of counts per pixel is shown by the colour scale.

low voltages. Capacitance-voltage tests on a 3D pad detector test structure also show this two-stage depletion behaviour [15]. The C-V curve initially drops very rapidly with bias, then it shows a distinct kink at 2.4V, beyond which the capacitance drops more slowly before reaching a minimum about 9V.

3.2 Spectral response and charge sharing

The Medipix2 3D detectors were tested with monochromatic X-rays on beamline B16 at Diamond Light Source [16]. The full experimental procedures and results from these tests are reported in [17]; here, just the spectral response results are described.

As discussed above, each hit on a Medipix2 detector is compared to a pair of thresholds, to determine whether the hit is accepted. So, an integral spectrum can be found by deactivating the upper threshold, and measuring the count rate on the detector as the lower threshold is varied. This can then be differentiated to find the differential spectrum of the detector.

One of the Medipix2 3D detectors, and a standard 300μm-thick planar Medipix detector, were used to make spectral measurements with beam energies of 12, 15 and 20keV. The beam was collimated to give a spot size smaller than the detector area, and the detectors were mounted on an adjustable stage so they could be moved in and out of the beam without adjusting it or switching it off. This ensured that the same flux was incident on the two detectors during the tests. While taking the spectra, the 3D detector was biased to 22V, and the planar detector to 100V, to ensure that both were fully depleted.

The results with the 15keV beam are shown in Fig. 7. Both detectors show a peak at the expected energy; each peak has been fitted with a Gaussian. The two detectors give very similar peak widths, indicating that their pixel noise and threshold dispersion are much the same. Both detectors also show lower-energy “hits”, which occur when charge is shared between two or more pixels. It can clearly be seen that the 3D detector has substantially less charge sharing and a larger signal peak than the planar detector, despite the 3D device’s lower bias voltage.

When charge generated by an X-ray is shared between two pixels, one pixel will see a hit above half the beam energy and the other will see a hit below. So, the relative numbers of charge-shared and non-charge shared photon hits can be found as indicated in Fig. 7. Averaged over the tests at the three energies, 23.4% of hits on the 3D detector were shared, compared to 39.5% on the planar detector. However, it was also found that the total hit rate (unshared plus shared) was 14% lower on the 3D detector. One of the downsides of the 3D structure is that hits occuring within the columns will be completely or partially lost. In these detectors, about 5% of the device volume will be occupied by the 10μm diameter columns, increasing to 10% if we include the heavily-doped regions around each column. Even taking this into account, the hit rate on the 3D detector is slightly lower than expected, though this could be explained by other effects such as differences in the substrate thicknesses (which are 300$\pm$15μm).

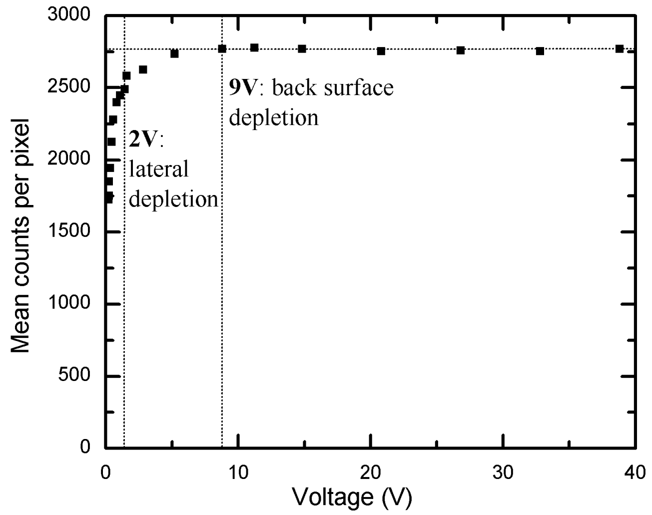

Figure 6: Count rate per pixel versus bias measured by a Medipix2 3D detector illuminated by a 60kVp X-ray tube, using a threshold energy of about 20keV. Reproduced from [14].

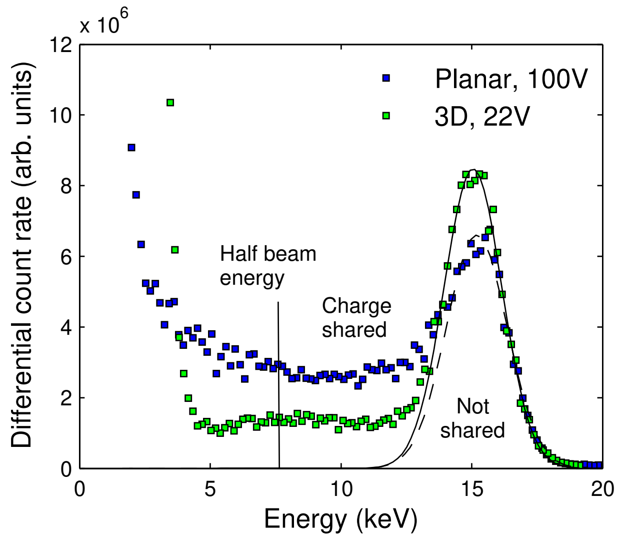

Figure 7: Spectral measurements from 3D and planar Medipix detectors tested with 15keV X-rays. Higher charge sharing can be seen on the planar detector.

4 Irradiated 3D strip detectors with LHC-speed readout electronics

The second set of devices we tested were four 3D strip detectors. These devices have an array of p- and n-type columns with 80μm spacing between columns of the same type. Rows of p-type readout columns are connected together by metal tracks, forming strips with an 80μm pitch. The strip detectors are relatively small, with 50 strips, each of which contains 50 readout columns, giving a strip length of 4mm. Around the edge of the array, p-type columns are connected to form a 3D guard ring.

Before connecting these devices to readout electronics, they were I-V tested, as described in [15]. All the strips tested in the four devices showed similar I-V characteristics, giving a current of around 100pA at 21°C and 50V bias. However, the guard ring currents were less consistent, with the lowest value being 0.03μA at 50V but with one device giving 20μA at just 10V. While guard ring current doesn't prevent the devices from operating, it increases power dissipation and can pose problems for bench voltage supplies. Guard currents are largely caused by surface leakage, so these results suggest there could be variations in the cut edges of the detectors.

C-V tests were also done on the strips, though the test setup could only bias one strip at a time, plus the bias columns, so the test conditions weren't ideal. These tests showed a capacitance of 5pF capacitance per strip, i.e. about 10pF/cm. This is large compared to standard strip detectors—for example, ATLAS SCT strips are designed to have less than 2.2pF/cm capacitance. The high capacitance is a downside of the small electrode spacing in a 3D detector.

4.1 DAQ setup for charge collection efficiency measurements

To test the charge collection efficiency of these detectors, a ^{90}Sr source was used as a source of betas. The test setup was triggered with a scintillator and photomultiplier tube placed behind the detector. A threshold was applied to the PMT signal to ensure that a trigger would only be generated if the beta had a high enough energy to act as a genuine minimum ionizing particle.

The data acquisition system was built using electronics from the LHCb experiment [18], in order to achieve a 25ns readout time. The strip detector was connected to a Beetle readout chip [19], which is used in the LHCb Velo and tracker. This chip can read out 128 channels at 40MHz, taking an analogue sample from each channel at each clock edge and storing it in an analogue pipeline. When a trigger occurs, all the samples from the appropriate time bin can be read out. The analogue sampling is useful for obtaining a signal spectrum, but since the betas arrive at random times with respect to the clock the sample won't always occur at the peak of signal pulse. To deal with this, extra trigger logic was added so that the trigger would only be generated for hits whose peak would coincide with the sampling time.

The detector and Beetle chip were mounted on a LHCb inner tracker hybrid—Fig. 8 shows a close-up of the module. The strip detectors produced by CNM were DC coupled, but the Beetle chip is designed for AC-coupled strips. So, an RC decoupling network chip had to be added between them. (Some tests were done with an unirradiated detector DC-coupled to the Beetle chip, on the basis that the chip should cope with a limited quantity of leakage current, but the experimental results were dubious.) The first attempt at adding an RC chip was unsuccessful; the network added a large amount of noise to each strip, and no signal could be read out. However, a second RC chip, provided by Jaakko Harkonen at the University of Helsinki, worked successfully. This chip had a resistor value of 1MΩ and a capacitance of 67pF.

Finally, the detector module was read out using the TELL1 readout board from LHCb [20]. Signal processing, including pedestal subtraction, linear common-mode noise subtraction and clustering, was done using the LHCb Vetra software package [21].

4.2 Collection efficiency after 5×10^{15} 1MeV-n$_{eq}$/cm^2 radiation damage

Before assembling the module, one of the strip detectors was irradiated to 5×10^{15} 1MeV-n$_{eq}$/cm^2, using neutrons from the TRIGA Mark II reactor at the Jozef Stefan Institute in Ljubljana. When the climate chamber containing the test setup was cooled to -25°C, the strip detector could be successfully biased to 200V. (Note that the temperature of the detector itself would have been higher during operation.) However, when the detector was cooled, some of its strips suddenly became much more noisy, independent of the bias applied to the detector. Although it's possible that the sensor itself might suffer from some temperature sensitivity, it's more likely that the problem was caused by the test setup; this is currently under investigation. These noisy strips were excluded during the data analysis.

When tested with betas at 200V, the detector produced the spectrum shown in Fig. 9. The spectrum has been fitted with a Landau distribution convolved with a Gaussian. The setup as a whole was calibrated by testing a 300μm, unirradiated, AC coupled n-on-p planar detector. Using the results from the reference detector, the most probable charge signal on the irradiated 3D strip detector was found to be 12800 electrons.

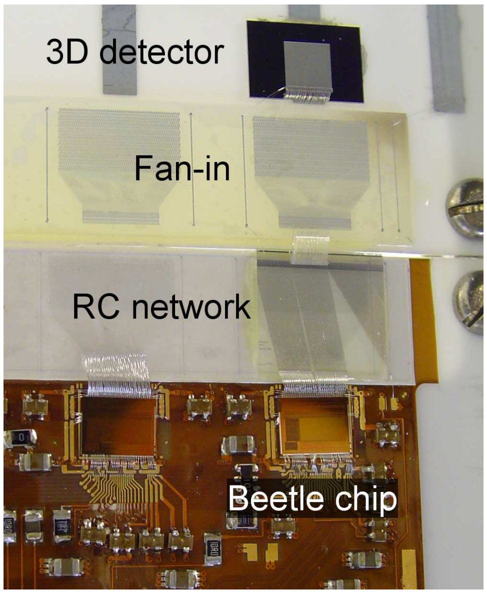

Figure 8: Close up of the 3D strip detector module used in the CCE tests.

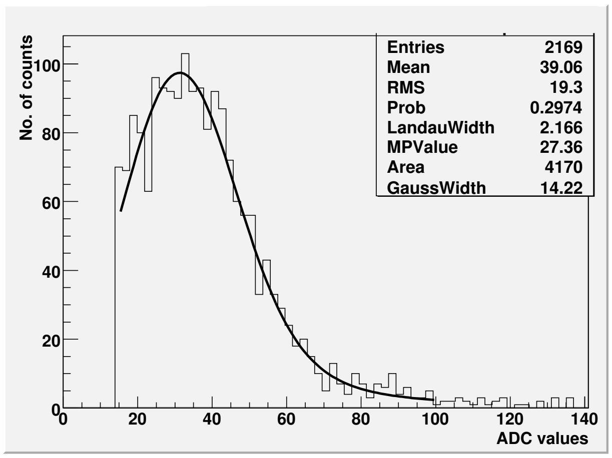

Figure 9: MIP spectrum measured from the 3D strip detector at 200V bias after irradiation to 5×10^{15} 1MeV-n_{eq}/cm^2. After calibration was applied, the most probable charge collection was found to be 12800 electrons.

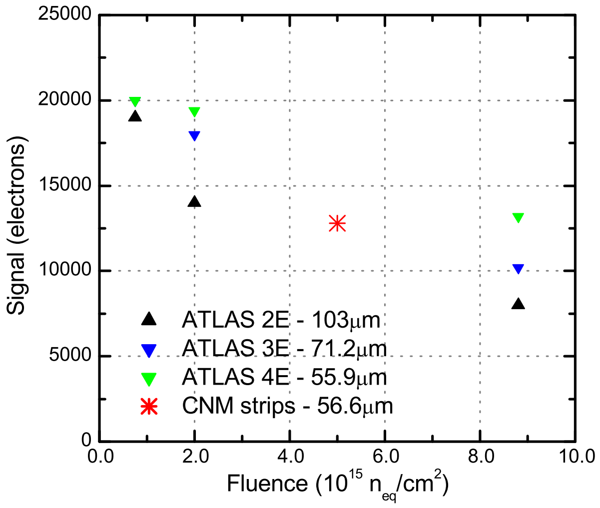

Figure 10: Comparison between the double-sided 3D strips from IMB-CNM tested here and full-3D test results reported in [22]. The signal collected from MIPs is plotted against irradiation fluence for each device.

4.3 Comparison with other 3D detectors

Figure 10 compares the collected signal from this double-sided 3D detector with results from full-3D detectors reported in [22]. These full-3D detectors were fabricated at the Stanford Nanofabrication Centre, and tested at Manchester. Like the double-sided detectors, they have 250μm long columns. However, the full-3D structure means that the substrate is 250μm thick. Also, these detectors used n-type readout and had a p-type substrate, whereas the detectors from CNM have p-type readout and n-type substrates. The full-3D devices used three different electrode layouts, all of which were compatible with the 400μm by 50μm pixel size of the ATLAS readout chip [23]. The different layouts used 2, 3 and 4 n-type readout columns per ATLAS pixel, and hence are referred to as 2E, 3E and 4E in the figure below. The resulting spacings between adjacent n- and p-type electrodes are also shown.

Overall, the charge collection from the double-sided 3D detector is comparable to the previous results from the full-3D detectors. The double-sided 3D detector has a relatively small electrode spacing, matching most closely to the "ATLAS 4E" configuration, but its collection signal is a bit lower. This could be because the double-sided 3D detector uses p-type readout rather than n-type. This means that the readout electrode collects holes, which have a shorter trapping distance than electrons due to their lower mobility.

It is important to note that the overall performance of a detector will depend not only on its charge collection, but also its noise level. 3D detectors have relatively high capacitances, which will tend to increase their noise. In particular, although making the electrode spacing smaller will improve the collection behaviour, this will also increase the capacitance [11].

5 New production run

Recently, IMB-CNM have finished a second production run of double-sided 3D detectors. This run consists of 8 p-type wafers with n-type readout and p-stop isolation, and 6 n-type wafers with p-type readout like the wafers in the first run. (Two more n-type wafers broke during fabrication.) Both sets of wafers contain more Medipix2 and strip detector devices. The p-type wafers with n-type readout also contain ATLAS pixel detectors—the ATLAS pixel readout chip is designed for n-type readout, so usable ATLAS devices weren't available from the first production run.

With proper characterisation of the signal and noise of the ATLAS pixel devices, it should be possible to make a fairer comparison between these double-sided 3D detectors and other technologies. The large number of strip devices in this run should also allow more thorough tests of radiation hardness at different fluences.

6 Conclusions

A set of double-sided 3D detectors have been successfully produced. Tests on Medipix2 pixel detectors have demonstrated that these devices have extremely low operating voltages, and that the 3D structure reduces charge sharing between pixels. Tests on irradiated strip detectors have shown that at a high damage fluence of 5×10^{15} 1MeV-n_{eq}/cm^2, the detectors still produce a collection signal of 12800 electrons, which is similar to the results from full-3D detectors.

Acknowledgment

The authors would like to thank Julien Marchal, Nicola Tartoni, Damien Barnett, Igor Dolbnya and Kawal Sawhney at Diamond Light Source for giving us access to beamline B16 at Diamond, and working with us on testing the Medipix2 detectors. Thanks also to Vladimir Cindro at the Jozef Stefan Institute in Ljubljana, for irradiating the strip detectors. This work has been supported by the Spanish Ministry of Education and Science through the GICSERV program "Access to ICTS integrated nano- and microelectronics cleanroom", and has been carried out in the context of the RD50 collaboration.

References

[1] S. I. Parker, C. J. Kenney, J. Segal, "3D - a proposed new architecture for solid-state radiation detectors", Nucl. Instr. and Meth A 395 (3) (1997) 328–343.

[2] V. A. Wright, W. D. Davidson, J. J. Melone, V. O'Shea, K. M. Smith, L. Donohue et al., "Three-dimensional Medipix - a new generation of X-ray detectors", IEEE Trans. Nucl. Sci. 52 (5) (2005) 1873–1876.

[3] V. Eremin, E. Verbitskaya, Z. Li, "Effect of radiation induced deep level traps on si detector performance", Nucl. Instr. and Meth A 476 (3) (2002) 537–549.

[4] F. Gianotti, "Physics opportunities of the LHC luminosity upgrade", Nuclear Physics B-Proceedings Supplements 147 (2005) 23–32.

[5] G. Gagliardi, "The ATLAS pixel detector: A hundred million channels vertex detector for LHC", Nucl. Instr. and Meth A 546 (1-2) (2005) 67–71.

[6] Y. Unno, "Silicon sensor development for the ATLAS upgrade for SLHC", Nucl. Instr. and Meth A 569 (1) (2006) 41–47.

[7] C. Da Via, J. Hasi, C. Kenney, V. Linhart, S. Parker, T. Slavicek et al., "Radiation hardness properties of full-3D active edge silicon sensors," Nucl. Instr. and Meth A 587 (2-3) (2008) 243–249.

[8] G. Pellegrini, M. Lozano, M. Ullan, R. Bates, C. Fleta, D. Pennicard, "First double-sided 3-D detectors fabricated at CNM-IMB", Nucl. Instr. and Meth. A 592 (1–2) (2008) 38–43.

[9] D. Pennicard, G. Pellegrini, M. Lozano, R. Bates, C. Parkes, V. O'Shea, V. Wright, "Simulation results from double-sided 3-D detectors", IEEE Trans. Nucl. Sci. 54 (4) (2007) 1435–1443.

[10] Synopsys Inc., Synopsys TCAD manuals, http://www.synopsys.com/products/tcad/tcad.html, (2007).

[11] D. Pennicard, G. Pellegrini, C. Fleta, R. Bates, V. O'Shea, C. Parkes, N. Tartoni, "Simulations of radiation-damaged 3D detectors for the Super-LHC", Nucl. Instr. and Meth. A 592 (1-2) (2008) 16–25.

[12] X. Llopart, M. Campbell, R. Dinapoli, D. S. Segundo, E. Pernigotti, "Medipix2: A 64-k pixel readout chip with 55μm square elements working in single photon counting mode", IEEE Trans. Nucl. Sci. 49 (5) (2002) 2279–2283.

[13] Z. Vykydal, J. Jakubek, S. Pospisil, "USB interface for Medipix2 pixel device enabling energy and position-sensitive detection of heavy charged particles", Nucl. Instr. and Meth. A 563 (1) (2006) 112–115.

[14] C. Fleta, D. Pennicard, R. Bates, V. O'Shea, C. Parkes, M. Lozano, G. Pellegrini, J. Marchal, and N. Tartoni, "X-ray detection with 3D Medipix2 devices", IWORID 2008 Conference Record. Submitted to Nucl. Instr. and Meth. A.

[15] D. Pennicard, G. Pellegrini, M. Lozano, C. Fleta, R. Bates, C. Parkes, "Design, simulation, production and initial characterisation of 3D silicon detectors," Nucl. Instr. and Meth. A, In Press, Corrected Proof, doi:10.1016/j.nima.2008.08.077

[16] Diamond Light Source, "B16 beamline plan", available at http://www.diamond.ac.uk/Beamlines/Beamlineplan/B16/default.h 2008.

[17] D. Pennicard, J. Marchal, C. Fleta, G. Pellegrini, M. Lozano, C. Parkes et al., "Synchrotron tests of a 3D medipix2 X-ray detector", submitted to Journal of Synchrotron Radiation, 2008.

[18] The LHCb collaboration, "The LHCb detector at the LHC", Journal of Instrumentation 3 (8) (2008) S08,005.

[19] S. Lochner, M. Schmelling, "The Beetle reference manual - chip version 1.3, 1.4 and 1.5" CERN report LHCb-2005-105 ; CERN-LHCb-2005-105, 2006.

[20] G. Haefeli, A. Bay, A. Gong, H. Gong, M. Muecke, N. Neufeld, O. Schneider, "The LHCb DAQ interface board TELL1", Nucl. Instr. and Meth. A 560 (2) (2006) 494–502.

[21] T. Szumlak, C. Parkes, "Description of the Vetra project and its application for the Velo detector," CERN report LHCb-2008-022. CERN-LHCb-2008-022, 2008.

[22] C. D. Via, E. Bolle, K. Einsweiler, M. Garcia-Sciveres, J. Hasi, C. Kenney et al., "3D active edge silicon sensors with different electrode configurations: Radiation hardness and noise performance", IEEE NSS Conference Record, Honolulu 2007.

[23] I. Peric, L. Blanquart, G. Comes, P. Denes, K. Einsweller, P. Fischer et al., "The FEI3 readout chip for the ATLAS pixel detector", Nucl. Instr. and Meth. A 565 (1) (2006) 178–187.